Accepted for publication in JAS

Theoretical analysis of the motion and evaporation of exhaled respiratory droplets of mixed composition

D. Parienta[1], L. Morawska[2], G.R. Johnson[2], Z.D. Ristovski[2], M. Hargreaves[2], K. Mengersen[2], S. Corbett[3],C.Y.H. Chao[4], Y. Li[5], D. Katoshevski[1*]

[1]Department of Biotechnology and Environmental Engineering, Ben-GurionUniversity of the Negev, Beer-Sheva, Israel
[2]QueenslandUniversity of Technology, Brisbane, QLD, Australia
[3]Centre for Public Health, Western Sydney Area Health Service, Sydney, NSW, Australia
[4]Department of Mechanical Engineering, TheHong KongUniversity of Science and Technology, Hong Kong SAR, China
[5]Department of Mechanical Engineering, TheUniversity of Hong Kong, Hong Kong SAR, China

[*]*Corresponding Author: davidk@bgu.ac.il*

Abstract

The dynamics of droplets exhaled from the respiratory system during coughing or talking is addressed. A mathematical model is presented accounting for the motion of a droplet in conjunction with its evaporation. Droplet evaporation and motion are accounted for under two scenarios: 1) A well mixed droplet and 2) A droplet with inner composition variation. A multiple shells model was implemented to account for internal mass and heat transfer and for concentration and temperature gradients inside the droplet. The trajectories of the droplets are computed for a range of conditions and the spatial distribution and residence times of such droplets are evaluated.

Introduction

The idea of infection via droplet nuclei was first introduced by Wells (Riley, 2001). Wells demonstrated droplet nuclei transmission of bovine TB in rabbits. The experiment was conducted by exposing the animals to air from the TB ward at the VA hospital in Baltimore. It was found that each animal had a single source TB, which fits with the idea of droplets diluted in large volumes if air. Wells (1934) had introduced the *Wells evaporation-falling curve of droplets* and found that droplets with an initial diameter of under 100μm will evaporate to create droplet nuclei before being removed by gravity (assuming initial height of 2m). Later studies refined these results.

Droplets emitted during cough, speech or sneeze collect different components from the respiratory tract before exiting. Effros et al. (2002) performed a chemical analysis of

condensates to obtain the composition. In addition towater, droplets were found to contain various salts and glycoproteins. The presence of additionalcomponents can indicate a disease, for example nitrotyrosine in a droplet can suggest asthma.

Several models have been suggested to describe the dynamics of a single aerosol particle emittedfrom the respiratory tract. All such models need to account for two processes:

1. Droplet motion

The motion of the droplet is determined by the forces acting upon it, including gravity, buoyancy and drag. Brownian motion can be neglected for droplets with diameter above 0.5μm.the size of the droplets also affects their motion, small droplets fall slower and also follow the streamlines more closely.

The velocity field in which the droplets travel is created by the exhaled air. The velocity of exhaled air depends on the method in which it was exhaled. For example, Chao et al. (2009) found from measurements that the average expiration air jet velocity was11.7m/s for coughing and 3.1m/s for speaking. The exhaled air formeda turbulent jet for which the Reynolds number wasevaluated using the velocity of the exhaled air and the diameter of the mouth.

2. Droplet evaporation

Droplets lose water through evaporation. Exhaled air exits at body temperature and high relative humidity (RH). As the droplets are in motion evaporation takes place as a function of their composition, their velocity relative to the gas, and the ambient conditions.

We address both aspects in the modeling to be presented later. A number of models have been presented previously in the literature.For example a model by Wang et al (2005) focused onSARS transmission via droplets. Thiswasbased on a 2D axisymmetric isothermal jet flow, assuming horizontal flow and uniform velocity distribution at the exit. Only the axial velocity component of the jet was used. The exhaled air was assumed to immediately reach equilibrium so that the temperature wasuniformly 293K. The relative humidity of the exhaled air wastaken to be 100%. To account for evaporation, Xie et al. (2007) revisited the Wells evaporation-falling curve in order to base it on a more accurate model, however, only inorganic salts were considered so the effect of salutes on droplet volume was negligible. The droplet temperature was assumed uniform and was found using energy balances. The evaporation was terminated when the size of the particles was under 3μm. The flow was

treated as a non-isothermal buoyant jet. A temperature field inside the jet was also taken into consideration.

Chao et al. (2009) modeled the jet-flow using the CFD software package FLUENT. The results show a mixing zone at a 10mm distance from the mouth where the temperature and RH remain unchanged. Since the exhaled air is considered to be at RH=100% approximately, and is cooled upon contact with the ambient air it was found that initially droplets undergo condensation rather than evaporation. The droplet composition was taken as a saline solution with NaCl content of 150mM (milli-Molar). The effect of the glycoproteins on the hygroscopic behavior was ignored.

In the current paper we demonstrate two models for droplet evaporation and relate them to droplet motion. The first model is of a uniform droplet with respect to temperature and concentrations of the solutes. The second model presents a multiple shells droplet with temperature and concentration gradients. In the course of the paper we first discussthe evaporation models and then droplet motion. The results of the calculations are then presented and analyzed.

The Model

Part 1 – Droplet Evaporation

Several models can be constructed to describe the evaporation of a droplet exhaled from the respiratory tract. We develop two options:

1) A uniform droplet, where the concentrations of the droplets components are distributed homogenously throughout its volume.Its temperature is uniform and may change only with time as the droplet travels through areas with different temperatures.

2) A droplet comprised of multiple shells, where each shell has different characteristics and mass and heat exchange occurbetween them, however each shell isitself considered to be uniform. The number of shellsdetermines the precision of the model.

Both models share some common characteristics. One of them is the mass flux from the droplet, which can be calculated from

$$\dot{m}_d = \frac{dm_d}{dt} = \rho_l 4\pi R_d^{\,2} \frac{dR_d}{dt} = 4\pi R_d^{\,2} K_d (\rho_{w\infty} - \rho_{ws}) \tag{1}$$

Where m_d is the mass of the droplet, R_d is the droplet radius, ρ_l is the density of water, K_d is the convective mass transfer coefficient, ρ_{ws} is the mass concentration of water at the surface of the droplet and $\rho_{w\infty}$ is the mass concentration of water vapor in the air surrounding the droplet.

Heat and water vapor are carried away from the droplet surface by forced convection. The convective mass transfer coefficient (K_d) and the convective heat transfer coefficient (h) are found by using the Ranz-Marshall correlations

$$Nu = \frac{D^* h}{k_g} = 2 + 0.6 Re_d^{\,1/2} Pr^{1/3} \tag{2}$$

$$Sh = \frac{D^* K_d}{D_g} = 2 + 0.6 Re_d^{\,1/2} Sc^{1/3} \tag{3}$$

Where D is the droplet diameter, D_g is the diffusion coefficient of water vapor in air, k_g is the thermal conductivity of air, Nu is the Nusselt number, Pr is the Prendtl number, Sh is the Sherwood number, Sc is the Schmidt number and Re_d is the droplet Reynolds number based on the velocity difference between droplet and gas.

Alternative correlations for finding the Nusselt and Sherwood numbers can be found in the literature, such as those based on Spalding mass and heat transfer numbers, e.g. the Abramzon and Sirignano model (Sazhin, 2006)

Model 1 – Uniform Droplet

This model is based on the assumption of a uniform droplet, meaning there are no gradients of either concentration or temperature inside the droplet. The only mass transfer is the evaporation of water from the droplet surface as described in eq. (1).

The temperature of the droplet changes according to

$$m_d C_l \frac{dT_s}{dt} = hA_s(T_\infty - T_s) + L_t \cdot \dot{m}_d \tag{4}$$

Where C_l is the heat capacity ofwater, T_s is the droplet temperature, A_s is the surface area of the droplet, T_∞ is the temperature of the air surrounding the droplet and L_t is the latent heat of water. The only changes to the droplet temperature are the result of convective heat transfer and heat loss due to evaporation.

Since water is the only component that evaporates the concentration of the different components changes according to

$$\frac{dm_w}{dt} = \frac{d}{dt}(\rho_w V_d) = \dot{m}_d \tag{5}$$

$$\frac{dm_{pr}}{dt} = \frac{d}{dt}(\rho_{pr} V_d) = 0 \tag{6}$$

$$\frac{dm_{sa}}{dt} = \frac{d}{dt}(\rho_{sa} V_d) = 0 \tag{7}$$

Where $m_i$is the mass of species *i*.Here and in the following equations: *i*stands for species, *w*-representing water, *pr* – glycoproteins and *sa* – salt ions. ρ_i is the mass concentration of species *i* (in gr/L) and V_d is the droplet volume.

The concentrations of the solutes were not restricted by any upper bound, therefore the saturation of the solution and crystallization of the solute are neglected.

The vapor pressure of water was found using Raoult's law and the Antoine equation (Dean, 1992). The Kelvin effect describing the effect of droplet curvature on the vapor pressure was

neglected because theeffectis not significant for droplets larger than 100 nm. The molar fraction of water was calculated from the following equation

$$X_w^{-1} = 1 + \frac{M_w(\rho_{sa} + \rho_{pr})}{M_s \rho_w} \quad (8)$$

Where X_w is the molar fraction of water, M_w is the molar weight of water and M_s is the average molar weight of the solutes (salt ions and glycoproteins) in the droplets.

The average molar weight of the solutes was calculated according to data from Nicas et al. (2005). Note that due to the high molecular weight of glycoproteins they have a small effect on the total molar concentration.

Model 2 – Multiple Shells Model

In this model the droplet is assumed to consist of multiple shells. This model enables us to account for gradients of concentration and temperature within the droplet. Each of the shells is treatedas uniform with respect to temperature and solute concentrations.The number of shells does not change during evaporation and all shells have identical thickness proportional to the diameter of the droplet.

Evaporation occurs at the outermost shell and the molar fraction of water needed for Raoult's law is calculated in the same manner as for a uniform droplet, but instead using values from the outermost shell.

In addition to evaporation from the outer shell, there are mass and heat transfers between the shells. The net mass transfer through each shell is proportional to the mass loss due to evaporation, while the flux of each species is determined by diffusion. The transient mass and temperature diffusion rates are found numerically, based on the following equations. Note that a positive flux is directed away from the center of the droplet.

For each of the shells

$$\frac{dm_{i,x}}{dt} = 4\pi\left(\frac{x-1}{Sh_n} R_d\right)^2 N_{i,x-1} - 4\pi\left(\frac{x}{Sh_n} R_d\right)^2 N_{i,x} \quad (9)$$

Where $m_{i,x}$ stands for the mass of component *i* in the shell*x* ranging from 1 to Sh_n, Sh_n is the number of shells, $N_{i,x}$ stands for the net mass flux of component i from shell *x* to shell *x+1*and R_d stands for the radius of the droplet.

The flux is the result of two elements: the evaporation of the droplet and diffusion.

$$N_{i,x} = J_{i,x} + \rho_{i,x} \frac{x}{Sh_n} \left| \frac{dR_d}{dt} \right| \tag{10}$$

Where $\rho_{i,x}$ is the concentration (in gr/L) of component *i* in shell *x* and $J_{i,x}$ is the diffusion flux of component *i* from shell *x* to shell *x*+1.

Note that this equation describes an evaporating droplet, in the case of condensation the concentration $\rho_{i,x}$ should be replaced by $\rho_{i,x+1}$.

The diffusion flux $J_{i,x}$ for the solutes is evaluated from

$$J_{i,x} = -\frac{D_i}{R_d / Sh_n} \left(\rho_{i,x+1} - \rho_{i,x} \right) \tag{11}$$

Where D_i is the diffusion coefficient of component *i*.

The diffusion flux of water is taken as complementary to the diffusion of the solutes.

The boundary conditions for the net flux are

$N_{i,0}=0$ (12)

As dictated by symmetry and

$$N_{w,Shn} = K_d (\rho_{ws} - \rho_{w\infty}) \tag{13}$$

$$N_{sa,Shn} = 0 \tag{14}$$

$$N_{pr,Shn} = 0 \tag{15}$$

The convective mass transfer coefficients for the mass flux inside the droplet are found from diffusion coefficients obtained from the Stokes–Einstein Relation and assuming *Nu*=2. It is important to note that since the Stokes-Einstein relation describes spherical molecules the diffusion coefficient for the glycoproteins can be overestimated. Electrostatic forces due to charged ions may have an effect on the diffusion rate, but were not included in this model.

The temperature of each shell can be found by using the following equations; taking into consideration heat transfer between the layers and heat convection from the droplet outer surface.

$$m_x C_l \frac{dT_x}{dt} = q_{x-1} 4\pi \left(\frac{x-1}{Sh_n} R_d \right)^2 - q_x 4\pi \left(\frac{x}{Sh_n} R_d \right)^2 \quad (16)$$

Where m_x is the mass of shell x, C_l is the heat capacity of water, T_x is the temperature of shell x and q_x is the heat flux from shell x to shell x+1.

The flux q_x is evaluated from

$$q_x = -\frac{k_w}{R_d / Sh_n} \left(T_{x+1} - T_x \right) \quad (17)$$

Where k_w is the thermal conductivity of water and T_x is the temperature of shell$x$. With boundary conditions:

$$q_0 = 0 \quad (18)$$

And

$$q_{Shn} = -h \cdot \left(T_\infty - T_{sh_n} \right) - \rho_L L_t \frac{dR_d}{dt} \quad (19)$$

Where h is the heat transfer coefficient determined by the Ranz-Marshall correlations, T_∞ is the temperature of the surrounding air and T_{sh_n} is the temperature at the surface of the droplet.

Part 2 – A Model for Droplet Motion

Air velocity

The air exhaled during a cough can be considered as a turbulent round jet (Xie, 2007). The flow is taken as a non-isothermal jet, but the effect of buoyancy is neglected. Instead, the jet is considered as exiting at an angle θ with respect to the horizontal. A turbulent jet is characterized by a potential core (also known as zone of flow establishment) in which the conditions along the centerline are identical to the conditions at the exit. Beyond the length of the potential core the axial velocity and temperature decline as a negative power of the distance x, x^{-1}. The temperature and axial velocity around the centerline are Gaussian in r/x. since the thermal diffusivity is larger than the kinematic viscosity (α=0.24cm^2/sec vs. ν=0.16cm^2/sec for air in 300K) the temperature distribution is expected to be flatter than the distribution of the axial velocity. The length of the potential core would also be shorter for temperature than for the axial velocity.

Droplet Motion

As the droplets are carried by the exhaled air, the forces considered in this model are gravity, buoyancy and drag. The contribution of other forces, such as added mass force, Basset history force and Brownian forces are neglected.

hence their momentum equations in the horizontal and lateral directions are written as:

$$\frac{d}{dt}(m_d v_z) = F_{D,z} \tag{20}$$

$$\frac{d}{dt}(m_d v_y) = F_{D,y} + m_d g(1 - \frac{\rho_a}{\rho_d}) \tag{21}$$

Where the drag F_D is calculated using Stokes law for Re_d<1, and by using a drag coefficient for Re_d>1.

The effect

Table 1 – parameters for the numerical simulations

Initial temperature (droplet and exhaled air)	T_0=310.15K
Ambient air conditions	T_r=298.15K, RH=50%Unless stated otherwise
Velocity of exhaled air (m/sec)	11.7 (cough), 3.9 (speak). Based on experiments by Chao et al. (2009)
Average molecular weight of the solutes	*Ms*=296.2gr/mol
Diffusion coefficient of water vapor in air	D_g=0.26cm^2/sec
Thermal conductivity (W/cm·K)	k_g=2.5·10^{-4} (air), k_w=6·10^{-3} (water)
Prandtl number	Pr=0.7205
Number of shells	Sh_n=8
Heat capacity of water	C_l=4.1813 J/gr·K

Results

The calculations according to the model, lead to the description of the dynamics of the exhaled droplets in terms of evaporation and spatial motion. The detailed quantitative analysis sheds light on the risk associated with the likelihood of spatial spread of a virus by those exhaled droplets. Results are first presented for evaporation and its dependence on a number of relevant parameters. The focus then shifts to droplet trajectories.

Uniform droplet

The evaporation of a droplet is characterized by a decline in droplet diameter and temperature from the initial diameter to the diameter of the nucleus and from the body temperature of the source to the temperature of the ambient air. The droplet is initially surrounded by the exhaled air which is characterized by high relative humidity and body temperature, but as the exhaled jet expands the conditions of the air surrounding the droplet change to those of the ambient air. During the evaporation the composition of the droplet varies rapidly. The evaporation process is affected by parameters such as the initial size of the droplet and the relative humidity of the ambient air.

Figure 1 shows the evaporation of several droplets with different initial diameters (20μm, 80μm, 320μm) and at different *RH* (50% and 80%). Figure 1(a) depicts the evolution of the droplet diameter and Figure 1(b) depicts the evolution of the droplet temperature. The droplets evaporating at the same *RH* (50%) exhibit similar behavior when the evolution of the diameter is plotted on dimensionless axis. The time of evaporation rises approximately by D^2 and the final diameter is proportional to the initial diameter.

Equ. (1) dictates that evaporation ends when the concentration of water vapor on the surface of the droplet is equal to the water vapor concentration in the ambient air, which is when the molar fraction of water is equal to the relative humidity. Therefore at high *RH* the droplets retain more water and the time of evaporation is longer, suggesting an increased risk at low humidity conditions.

The hygroscopic growth factor (HGF) is the ratio of droplet diameter in equilibrium to the diameter of a dry droplet. As expected, the HGF increases with an increase in *RH*. This ratio is not dependent on droplet size, but only on *RH* and the initial composition of the droplet. For high values of *RH* the HGF exceeds the ratio of the initial diameter to dry diameter, meaning that condensation will occur rather than evaporation. This is also true for the initial moment when the droplet is surrounded by the exhaled air, as was found by Chao et al.

(2009). For small enough values of *RH*, there is almost no water left in the droplet after evaporation, resulting in a solid or gel-like particle.

The temperature decrease is caused by both convective heat transfer and heat loss due to evaporation. Figure 1(b) shows a rapid decrease in droplet temperature during evaporation and a rise to ambient air temperature after evaporation. The decline in temperature is more rapid for large droplets because of the smaller surface to volume ratio. The difference under different *RH* conditions is caused by the difference in evaporation rate discussed before.

The change in concentrations is depicted in Fig. 2. As expected we see a decrease in water concentration and an increase in the concentration of solubles during evaporation. When plotted against dimensionless time the results indicate a behavior similar to that of the diameter. The final concentrations are determined by the *RH* and are independent of the droplet's size.

Convective heat and mass transfer from the droplet are the result of velocity difference between the droplet and the surrounding air. Convective heat and mass transport were added to the model based on the Ranz-Marshall correlations. In order to test the role of convective transport the Sherwood and Nusselt number are set to $Sh=2$ and $Nu=2$. Figure 3 shows the results for two droplets with initial diameters of 20μm and 320μm. It can be seen that for a 20μm droplet there is effectively no difference between evaporation based on convective transport or non-convective transport. In contrast it can be seen that for a 320μm droplet, convective transport accelerates the rate of evaporation. This is caused as a result of the different relative velocities of droplets of different sizes. As expected small droplets tend to follow the streamlines more closely than large droplets, maintaining a velocity similar to that of the surrounding air, and therefore are less affected by convective transport.

Multi-Shells Droplet

The evaporation rate of uniform and multi-shells droplets with different initial diameters is presented in Fig. 4. Comparing the two models, we can see that the multi-shells droplet predicts a two-stage evaporation process. The first stage is characterized by a rapid decline in the droplet diameter, very similar to that of a uniform droplet. The second stage is characterized by slower decline until evaporation ends.

The change in concentrations of the different components is shown in Fig. 5 for a 20μm droplets. We can see that evaporation is characterized as having two stages. In the first stage we see a fast decline in water concentration, coupled with an increase in solute concentrations, in the outer shell while there is little to no change in the inner shells. This is

caused by the difference between the fast diffusion of water vapor in air compared to the slower diffusion in liquids. In the second stage the gradient in concentrations between the shells causes a diffusion of solutes from the outer parts of the droplet inside and of water towards the outer shell, which causes a rise in solutes concentrations in the inner shells. Water from the inner shells that reach the surface causes evaporation to continue. The droplet concentrations profile is presented in Fig. 6. As expected we can see that the change in concentrations occurs first at the outer shells and moves towards the center of the droplet. The profile for salt ions depicted in Fig. 6(b) is more moderate than the profile for proteins depicted in Fig. 6(c), since salt ions are smaller than proteins and have a higher diffusion coefficient.

The concentrations of salt ions and gylcoproteins can vary between different droplets. We have examined three possible concentrations: an average droplet, a droplet with high concentrations and a droplet with low concentrations, all 20μm in diameter. It was found that the higher the initial concentration of solutes is, the longer it takes before the droplet reaches a uniform distribution. Similarly to the uniform model, the higher the concentration of solutes the larger the droplet is at the end of evaporation. It is also possible to consider a situation in which the components of the droplet are not distributed uniformly at the beginning of the evaporation. We tested two 20μm droplets: A droplet in which the concentrations are higher at the outer shells (increasing concentrations) and a droplet in which the concentrations are higher at the center (decreasing concentrations), all droplets having same net concentration. Because the initial concentrations profile is not uniform diffusion starts earlier than in previous cases. There is a decrease in salt concentrations in the middle shells as a result of diffusion to the center. The center and middle shells reach temporary equilibrium which is disrupted by the evaporation in the outer shells.

Droplet trajectories

The motion of various droplets is shown in Figs. 7 and 8. Fig. 7(c) depicts the trajectories for droplets with different initial diameters during cough and Fig. 8(c) depicts the trajectories for droplets during speech. The flow velocity was taken to be 11.7m/sec for cough and 3.9m/sec for speech (Chao et al. 2009). It can be seen that large droplets are removed by gravity after a short distance and time, while small droplets can remain suspended for prolonged periods. Droplets reach longer distances during cough because of the higher initial velocity.

It can be seen that the large droplets reach their maximal horizontal distance very quickly, thereafter the effect of the air velocity is negligible and the droplet settles at a terminal velocity. As seen in Fig. 7(b) the time of fall is shorter for larger droplets, as a result of their

terminal velocity. The maximal horizontal distance is influenced by two factors: the terminal velocity and the momentum of the droplet. Because of that we see a minimum at around ~100μm (Fig 7(c)).

Small droplets reach a longer horizontal distance, which is expected since small droplets have lower terminal velocities and hence are closer to the jet centerline where the axial velocity is at its highest. A 2μm droplet not only reaches a longer distance and remains suspended for a longer period it also retains a certain horizontal velocity until it settles. Therefore it can be expected that changes in the jet characteristics would have a greater effect on smaller droplets.

Concluding Remarks

In this paper we present a mathematical model that describes the dynamics of exhaled droplets. It is an additional effort, in the modeling point of view, complimenting the findings of an intensive campaign conducted recently (and published in JAS) by the authors to investigate the properties of expiratory aerosols (Morawska et al., 2009, and Chao et al., 2009).

The model is used to analyze the effect of environmental conditions, flow and droplet characteristics on the evaporation of the droplets and subsequently their motion. We present two models for evaporation of droplets containing non-volatile components: the simpler uniform droplet and the more refined multi-shells droplet. Analysis of the multi-shells model predicts that the evaporation of respiratory droplets is a two-stage process.

In terms of droplet dynamics we show that there is a clear distinction between large droplets which tend to fall within several meters, dependent on the initial velocity of the exhaled air, and small droplets that can stay suspended and reach longer distances. On a smaller scale, other variables such as the ambient relative humidity or the composition of the droplet also play a role in determining the distance the droplet travels. These results correspond with the distinction between transmission by droplet contact and airborne transmission routes.

The results presented here can serve together with the corresponding reported measurements in assessing the risk associated with the transmission of airborne diseases and assist in designing solutions to minimize this risk in controlled environments.

References

Chao, C.Y.H., Wan, M.P., Morawska, L., Johnson, G.R., Ristovski, Z.D., Hargreaves, M., Mengersen, K., Corbett, S., Li, Y., Xie, X., &Katoshevski, D., (2009). Characterization of Expiration Air Jets and Droplet Size Distributions Immediatle at The Mouth Opening, Journal of Aerosol Science, 40, 122-133.

Dean, J.A., (1992). Lange's handbook of chemistry, 14th edition, New York : McGraw-Hill.

Effros, R.M., Hoagland, K.W., Bosbous, M., Castillo, D., Foss, B., Dunning, M., Gare, M., Lin, W., & Sun, F., (2002). Dilution of Respiratory Solutes in Exhaled Condensates, American Journal of Respiratory and Critical Care Medicine, 165 (5), 663-669.

Morawska, L., (2006). Droplet Fate in Indoor Environments, Or Can We Prevent the Spread of Infection?, Indoor Air, 16 (5), 335-347.

Morawska, L., Johnson, G.R., Ristovski, Z.D., Hargreaves, M., Mengersen, K., Corbett, S., Chao, C.Y.H., Li, Y., Katoshevski, D., (2009). Size Dstribution and Stes of Origin of Droplets Expelled from The Human Respiratory Tract During Expiratory Activities, Journal of Aerosol Science, 40 (3), 256-269.

Nicas, M., Nazaroff, W.W., Hubbard, A., (2005). Toward Understanding the Risk of Secondary Airborne Infection: Emission of Respirable Pathogens, Journal of Occupational and Environmental Hygiene, 2 (3), 143-154.

Ranz, W.E. & Marshall, W.R., (1952). Evaporation from Drops, Part I, Chemical Engineering Progress, 48, 141–146.

Riley, R.L., (2001). What Nobody Needs to Know About Airborne Infection, American Journal of Respiratory and Critical Care Medicine, 163 (1), 7-8, JAN 2001

Sazhin, S.S., (2006). Advanced Models of Fuel Droplet Heating and Evaporation, Progress in Energy and Combustion Science, 32 (2), 162-214.

Wang, B., Zhang, A., Sun, J.L., Liu, H., Hu, J., Xu, L.X., (2005). Study of SARS Transmission via Liquid Droplets in Air, Journal of Biomechanical Engineering-Transactions of the ASME, 127 (1), 32-38.

Wells, W.F., (1934). On Air-Borne Infection. Study II. Droplets and Droplet Nuclei, American Journal of Hygiene, 20, 611–618.

Xie, X., Li, Y., Chwang, A.T., Ho, P.L., Seto, W.H., (2007).How Far Droplets Can Move in Indoor Environments - Revisiting the Wells Evaporation-Falling Curve, Indoor Air, 17 (3), 211-225.

List of figures

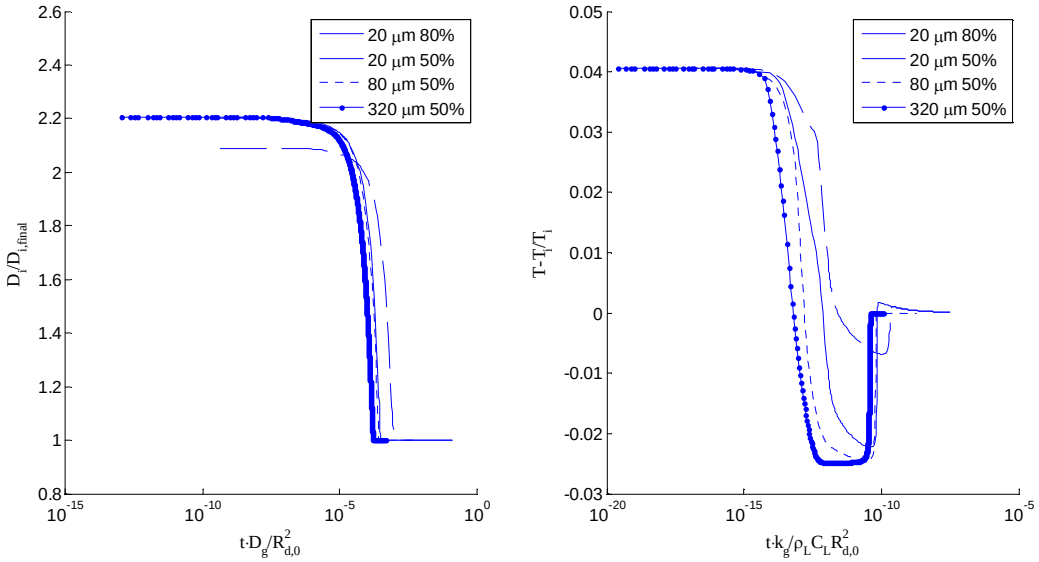

Figure 1 – Evolution of (a) Droplet diameter and (b) Temperature for a uniform droplet with different initial diameters and RH.

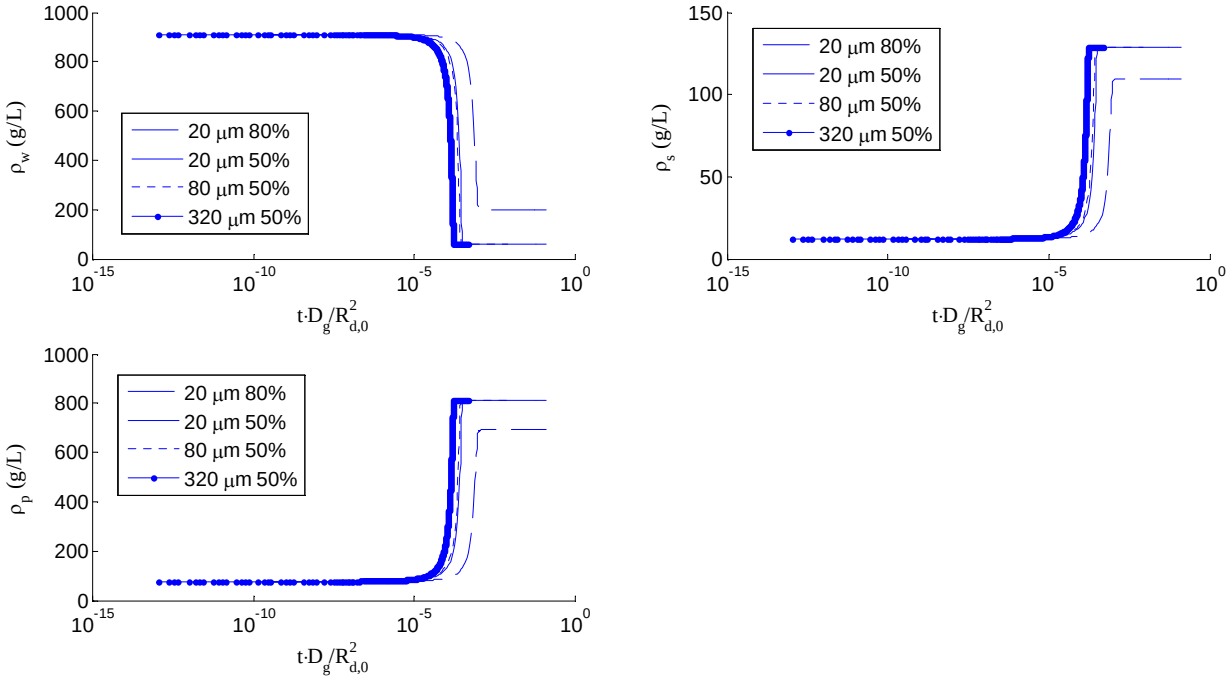

Figure 2 – Concentration of components (a) Water (b) Salts and (c) Proteins during evaporation of a uniform droplet with different initial diameters and RH.

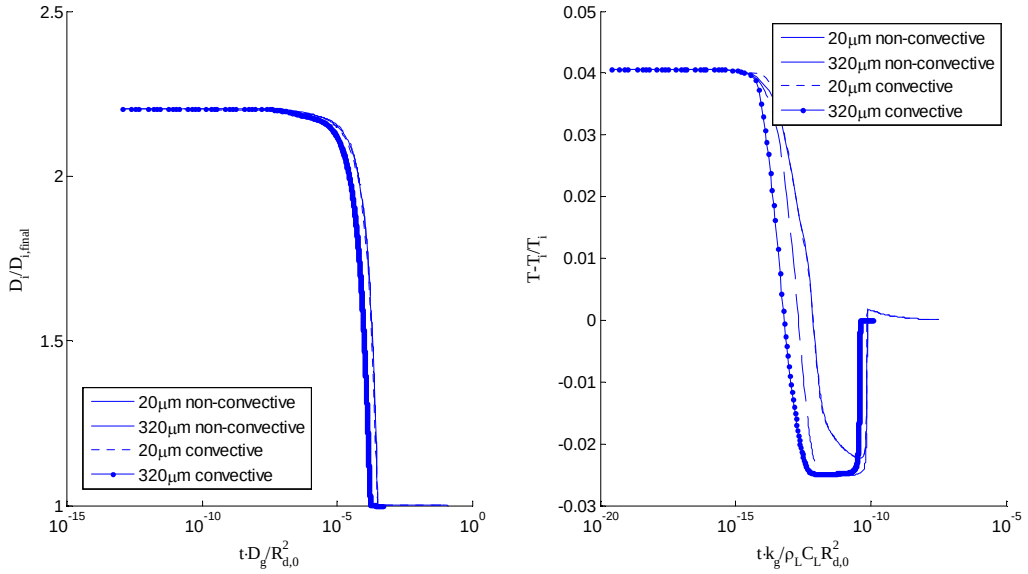

Figure 3 – (a) Droplet diameter and (b) Temperature for 20 μm and 320 μm uniform droplets with and without convective heat and mass transport.

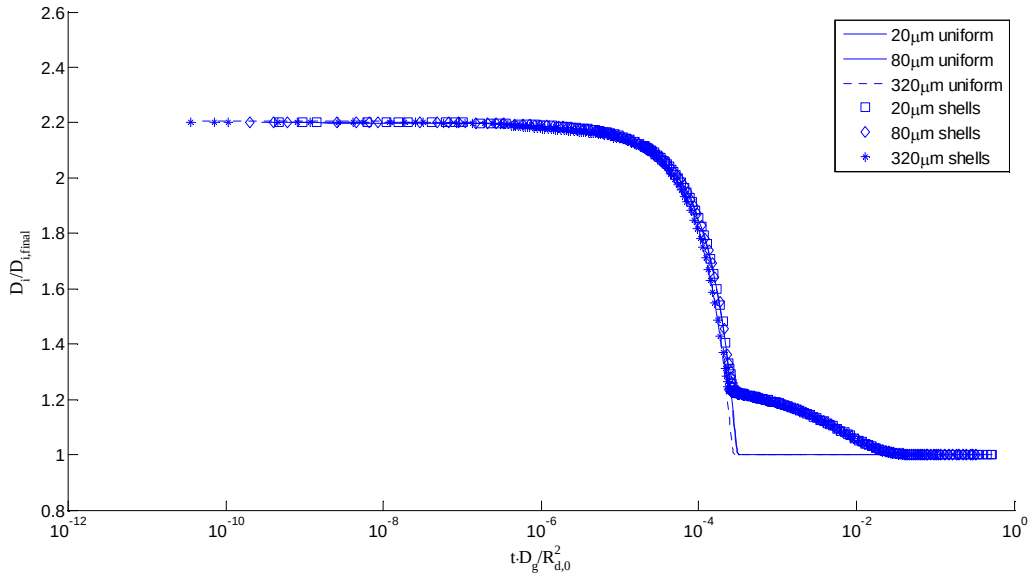

Figure 4 - Droplet evaporation for uniform and multiple shells droplets with different initial diameters.

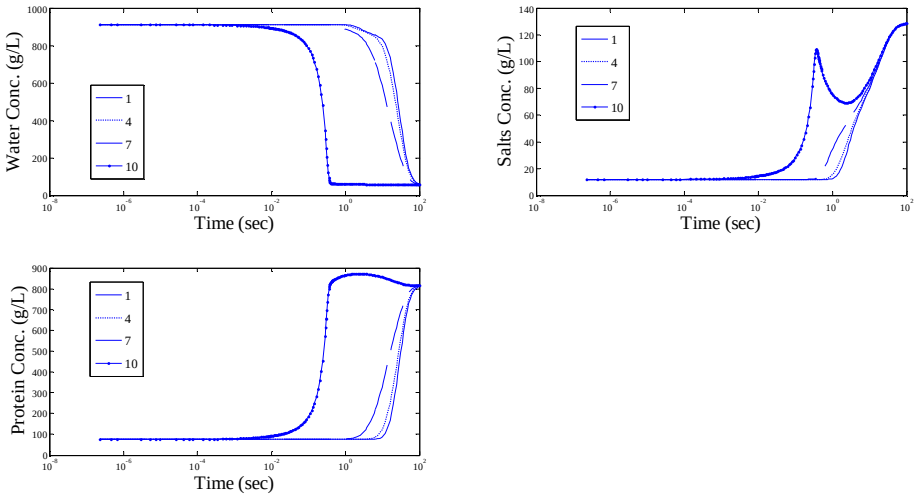

Figure 5 – Change in Concentrations of (a) water, (b) salts and (c) proteins in several shells for a 20μm droplet.

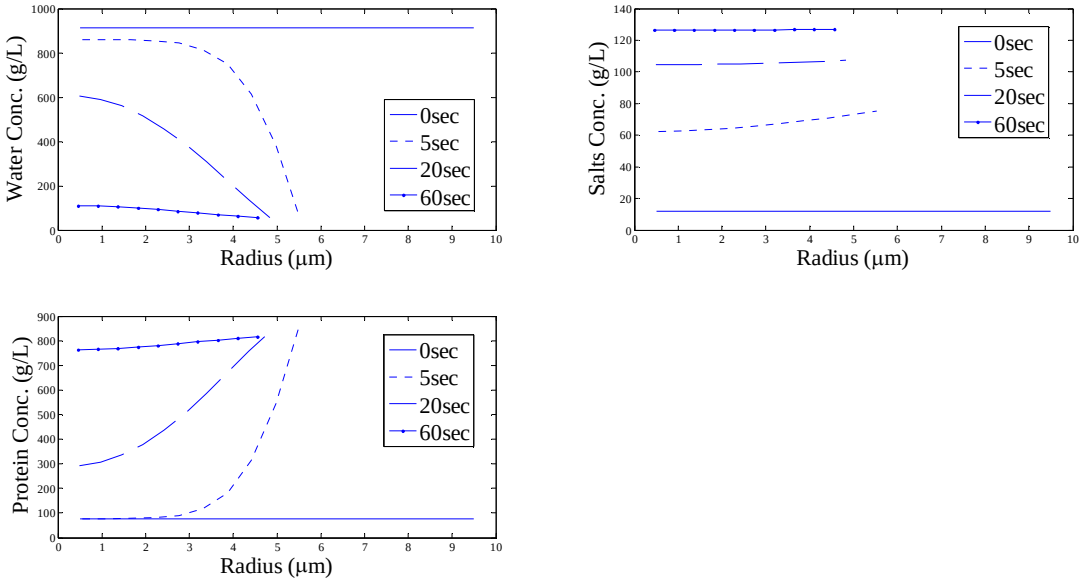

Figure 6 – Droplet concentrations profile for (a) water, (b) salts and (c) proteins at several times for a 20μm droplet.

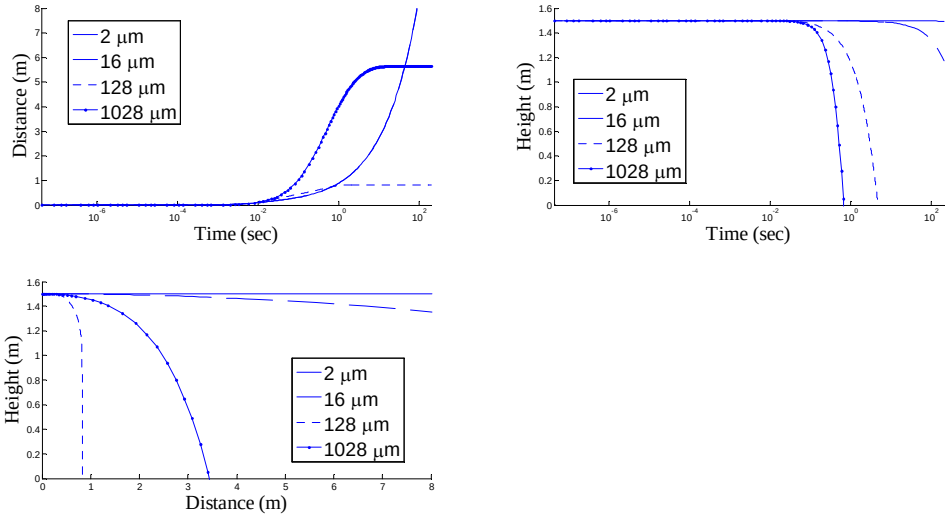

Figure 7 – Motion of droplets with various initial diameters during cough, initial flow velocity 11.7m/sec. (a) Horizontal distance vs. time (b) Droplet height vs. time (c) Trajectory of the droplet.

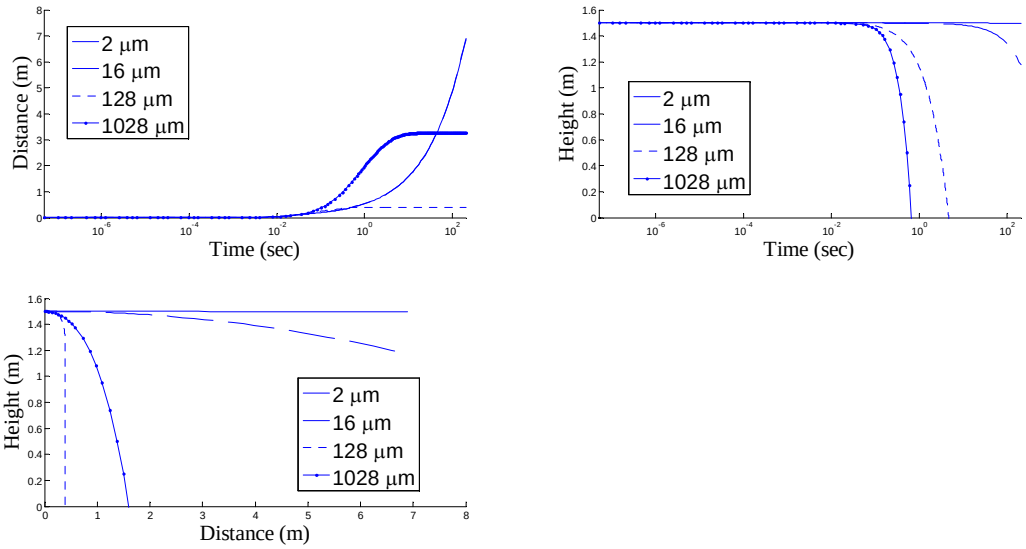

Figure 8 - Motion of droplets with various initial diameters during speech, initial flow velocity 3.9m/sec. (a) Horizontal distance vs. time (b) Droplet height vs. time (c) Trajectory of the droplet.